Sixth International Symposium on Turbulence and Shear Flow Phenomena
Seoul, Korea, 22-24 June 2009

Comparison of experiment and direct numerical simulation in turbulent channel flow

J. P. Monty & M. S. Chong
Department of Mechanical Engineering,
University of Melbourne, VIC, 3010, Australia
nhu@unimelb.edu.au

ABSTRACT

The numerical simulation of the turbulent flow between parallel plates has advanced rapidly over the past two decades. Numerical simulations are increasingly important as the Reynolds number achievable (due to computing power) increases over time. Although simulation Reynolds numbers now overlap with reliable laboratory experimental capability, there are no detailed comparisons with the similar experimental case: the flow in a high aspect ratio rectangular duct. As such, this paper seeks to compare a highly regarded, well-documented numerical simulation by (2) with new, highly accurate experimental data from the channel flow facility at the University of Melbourne.

INTRODUCTION

Progress in the Direct Numerical Simulation (DNS) of turbulent flow between parallel plates has increased dramatically in recent decades. At this point in time, DNS studies have reached similar Reynolds numbers to that achievable in the laboratory ($Re_\tau = U_\tau h/\nu \approx 2000$, where U_τ is the friction velocity, h is the channel half-height and ν is the kinematic viscosity). Notable examples are found in references (7; 2; 4; 8).

Despite the fact that DNS solves the Navier-Stokes equations exactly, there are still opportunities for inaccuracy to enter the results through choice of parameters such as grid-spacing, box size, time-steps, etc. As such, it is imperative that simulations are compared with experiment for validation. This is particularly pertinent for fundamental flows where parameters can be matched with those of laboratory studies. However, a detailed comparison between numerically simulated and experimental turbulent channel flow has not been provided in the literature to date. This is undoubtedly due to the lack of reliable, well-documented and highly detailed experimental data available. It is, therefore, the aim of this paper to compare the mean velocity, turbulence intensity and one-dimensional energy spectra of a well-documented DNS and a new laboratory turbulent channel flow at 'high' Reynolds number. The $Re_\tau = 934$ DNS simulation by Del Alamo *et al.* (2004) has been selected for comparison with the laboratory measured data.

EXPERIMENTAL & NUMERICAL DETAILS

The channel flow facility at the University of Melbourne uses air as the working fluid and has a maximum bulk velocity, $U_{b(max)} \approx 30$ ms^{-1}. The channel has half-height, $h = 50$ mm and width of 1170mm so that the aspect ratio is 11.7:1, giving a central channel volume of nominally two-dimensional flow at least 600mm (or $12h$) in width. Further details are given in (10). Single point hot-wire measurements were made at 52 wall-normal locations with an automated traversing system with negligible backlash and capable of 5 μm movements. The hot-wire had a relatively small sensing length of 0.5 mm, corresponding to $8.5\nu/U_\tau$ in wall units. The streamwise pressure gradient was used to determine friction velocity. A Kármán number of $Re_\tau = 1040$ was achieved with a bulk velocity of 6.130 ms^{-1}, $U_\tau = 0.304$ ms^{-1} and $\nu = 1.477\times10^5$ m^{2}s^{-1}. It is estimated that there is at most 1% error in hot-wire measured mean velocity and 2% in turbulence intensity. Due to measurement errors very near the wall, data below $y^+ \approx 8$ were discarded and no comparisons are drawn from data below $y^+ = 15$.

The DNS data set has been well-documented, having a Reynolds number, $Re_\tau = 934$ and a box-size of $8\pi h \times 3\pi h \times 2h$ with a grid of $3072\times2304\times385$ points. The grid spacing in the x and z directions are 7.6 and 3.8 wall units, respectively (1 wall unit $= \nu/U_\tau$, x is the streamwise direction, y, the wall-normal and z, the spanwise direction).

MEAN STATISTICS

Figure 1 shows mean statistics for the two data sets. The overall agreement is clearly very good. When plotted with inner-scaling, attention is drawn to the collapse of the data very near the wall ($y < 100\nu/U_\tau$, say). Here we observe only a small attenuation in the experimental turbulence intensity. This is undoubtedly due to the spatial averaging of the hot-wire, which had a sensing length of 8.5 wall units. While this is a relatively short wire, it is still twice the grid spacing of the DNS.

The outer-scaled data also show very good collapse. The turbulence intensity shown in figure 1*d* also illustrates the mismatch in Reynolds number between the DNS and experiment, especially when compared with 1*a*. That is, although the data collapse well near the wall with inner-scaling, outer-scaling improves collapse far from the wall and reduces the agreement near the wall, indicating a Reynolds number discrepancy. The Reynolds number of the experiment is approximately 10% higher than the DNS, although this mismatch will not affect any of the conclusions drawn.

The maximum difference in mean statistics between data sets occurs very near the wall in the mean velocity ($\sim 4\%$). However, all discrepancies are within the scatter of experimental data from different facilities taken over many decades. Although there is limited experimental channel flow data for comparison, the author's experience with zero-pressure-gradient boundary layer data has been that there are signficant unresolved differences between data sets from different laboratories. As such, it is concluded that the mean statistics show no significant differences — a result that should encourage all wall-turbulence researchers, experimental or numerical.

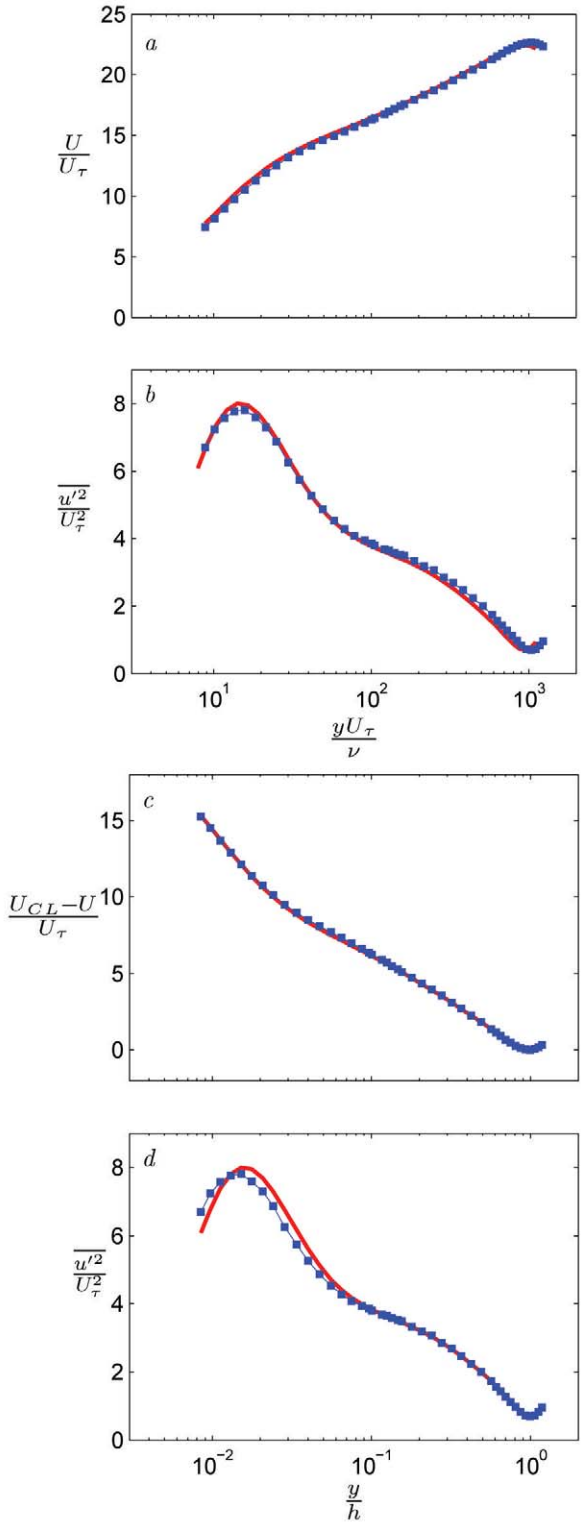

Figure 1: (*a*) Inner-scaled mean velocity profiles and; (*b*) associated broadband turbulence intensity; (*c*) Outer-scaled velocity defect profiles and; (*d*) associated broadband turbulence intensity. Symbols represent experimental data, while solid lines are the DNS results.

ENERGY SPECTRA

In recent years there have been a number of groundbreaking studies on the large-scale structure of wall-turbulence, e.g. (5; 2; 9; 3). The important findings have largely resulted from spectral analyses of the turbulent velocity fields. Therefore, it is important to compare the experimentally determined spectra with the numerical. Since the hot-wire gives a temporal velocity trace and the numerical data give a spatial velocity field, it is necessary to assume a convection velocity at each distance from the wall. Consistent with previous investigations, we choose to infer the spatial spectrum from the temporal for the experimental data to compare with the spatial spectrum from the DNS. For this purpose the local mean velocity is chosen as the convection velocity throughout this section.

Figure 2 presents pre-multiplied spectra (energy spectra) for both flows at a variety of wall-distances. In figure 2*a*, wavelength is scaled with inner variables and data from $y^+ = 15 - 100$ are presented. The agreement is very good overall with both data sets showing very similar shaped spectral distributions. In figure 2*b*, wavelength is scaled with the channel half-height since data is presented from the outer region, $y = 0.15 - 0.7h$. Far from the wall, the spectra from the two data sets agree quite well again, particularly beyond the log region. One notable difference is that there is a secondary peak energy of $k\Phi_{11} \approx 0.7U_\tau^2$ at a wavelength, $\lambda_x \approx 10h$ in the log region for the experimental data. A similar spectrum is observed in boundary layers at this wall location (5), although the secondary peak is at shorter wavelengths. At the edge of the log region, $y/h = 0.15$, both data sets show close agreement for $\lambda_x < 4h$. However, there appears to be an appreciable attenuation of energy in the DNS in the vicinity of $\lambda_x = 10h$; the secondary 'peak' is more like a shoulder. This missing secondary peak in the DNS represents only a small fraction of the total energy, but Guala *et al.* (3) found that features of the wavelengths discussed here are responsible for up to half of the Reynolds shear stress in the log region, suggesting the missing energy could be a concern. Hutchins and Marusic (6) and del Alamo *et al.*(1) also show that these structures have a 'footprint' near the wall, suggesting they are significant contributors throughout the flow. Since the wavelengths where the DNS and experiment differ most (peaking at $\lambda_x \approx$12–14h) are so close to the box length of the DNS (25.13h), it is logical to suspect an insufficient box size as the source of the discrepancy.

It is difficult to develop an overall view of the spectral behaviour from figure 2 alone. Recently, Hutchins & Marusic (5) have shown a more convenient way to show the spectral behaviour with wall-distance using the spectra map as shown in figure 3. Here we plot contours of pre-multiplied spectra against wavelength and wall-distance. Inner-scaling is used here, although very little difference is observed with outer-scaling, since the Reynolds numbers of the two data sets are sufficiently close. Once again, the overall picture is very similar for both flows, although the energy discrepancy in the log region at long wavelengths is now clearly evident ($y^+ \approx 100, \lambda_x^+ \approx 10^4$). A closer look also reveals strange differences in the large-scales very near the wall ($y^+ < 50$). It appears that the DNS exhibits more energy near the wall than the experiment. This is difficult to understand, particularly since the same scales are much more energetic in the log region for the experiment. If the large-scale energy near the wall is the footprint of the log region structures, as suggested by Hutchins & Marusic (5), then the experimental data should show more energy near the wall, not less. One

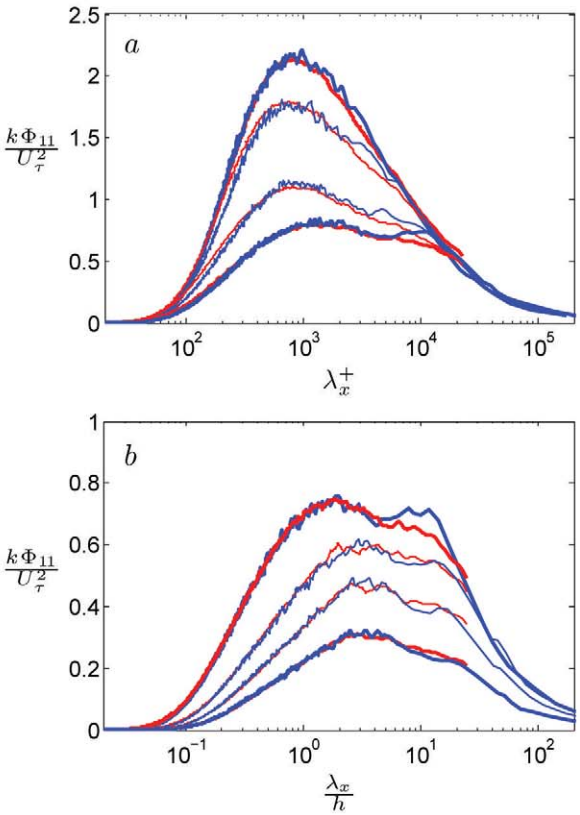

Figure 2: Pre-multiplied power spectral density, $k\Phi_{11}/U_\tau^2$, plotted against non-dimensional wavelength, $\lambda_x = 2\pi./k$. (a) Spectra near the wall shown with inner-scaling, $y^+ = 15$ – 100; (b) Spectra further from the wall with outer-sclaing, $y = 0.15 - 0.7h$. Experimental data in blue, DNS in red. Heavy lines are data at $y^+ = 15, 40$ and $y = 0.15h, 0.7h$.

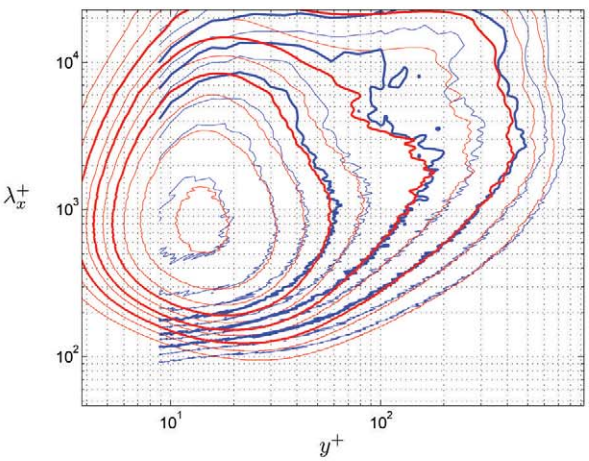

Figure 3: Spectra contour map. Experiment in blue, DNS in red. Contour levels are 0.30, 0.40, **0.50**, 0.6, **0.72**, 0.85, **1.00**, 1.20, 1.50 and 2.02 (from outermost to innermost).

possibility is that the choice of a constant convection velocity to infer the spatial spectrum from experimental data is incorrect.

ENERGY REDISTRIBUTION DUE TO CONVECTION VELOCITY VARIATION

It is trivial to modify convection velocity by a constant factor for any given wall-distance. However, for a scale-dependent convection velocity modification, greater care is needed in order to ensure that the pre-multiplied spectra remains the *energy* spectra; i.e., the area under the pre-multiplied spectra remains the turbulence intensity. The following analysis shows that a non-trivial redistribution of the energy is required to maintain the physical relevance of the energy spectrum.

Let us begin with the initial scaling of the energy spectra, which assumes a constant convection velocity (the local mean is chosen):

$$\overline{u'^2} = \int \Phi_{11}(k)dk = \int k\Phi_{11}(k)d(\ln(k)), \tag{1}$$

where k is the associated streamwise wavenumber and Φ_{11} is the power spectral density (PSD).

$$\overline{u'^2} = -\int k\Phi_{11}(\lambda_x)d(\ln(\lambda_x)) \tag{2}$$

Here we define the wavelength associated with the PSD as

$$\lambda_x = \frac{2\pi}{k} = \frac{U_c}{f}, \tag{3}$$

where U_c is the convection velocity and f is the frequency associated with the PSD. Assuming we start with a convection velocity equal to the local mean, U_l, the modified wavelength is defined by

$$\lambda_x c(\lambda_x) = c(\lambda_x)\frac{U_l}{f}, \tag{4}$$

so that $c(\lambda_x)$ is simply a function representing an amplification of the convection velocity above or below the local mean. So

$$\overline{u'^2} = -\int k\Phi_{11}(\lambda_x c(\lambda_x))d\left(\ln\left[\lambda_x c(\lambda_x)\right]\right), \tag{5}$$

however, we would like to know the relationship between $k\Phi_{11}(\lambda_x)$ and $k\Phi_{11}(\lambda_x c(\lambda_x))$. This is easily achieved:

$$\overline{u'^2} = -\int \frac{d(\ln\lambda_x)}{d(\ln\left[\lambda_x c(\lambda_x)\right])} k\Phi_{11}(\lambda_x)d\left(\ln\lambda_x\right)\frac{d(\ln\left[\lambda_x c(\lambda_x)\right])}{d(\ln\lambda_x)}. \tag{6}$$

Now the derivative of the two logarithms is all that is needed:

$$\frac{d(\ln\left[\lambda_x c(\lambda_x)\right])}{d(\ln\lambda_x)} = \frac{d(\ln\lambda_x)}{d(\ln\lambda_x)} + \frac{d(\ln c(\lambda_x))}{d(\ln\lambda_x)} \tag{7}$$

$$= 1 + \frac{d(\ln c(\lambda_x))}{dc(\lambda_x)} \times \frac{dc(\lambda_x)}{d\lambda_x} \times \frac{d\lambda_x}{d(\ln\lambda_x)} \tag{8}$$

$$= 1 + \frac{c'(\lambda_x)\lambda_x}{c(\lambda_x)}. \tag{9}$$

Inserting this result into equation 6 gives

$$\overline{u'^2} = -\int \frac{c(\lambda_x)}{c'(\lambda_x)\lambda_x + c(\lambda_x)} k\Phi_{11}(\lambda_x)d(\ln\left[\lambda_x c(\lambda_x)\right]), \tag{10}$$

so that the energy redistribution function, $G(\lambda_x)$ is defined as

$$G(\lambda_x) = \frac{c(\lambda_x)}{c'(\lambda_x)\lambda_x + c(\lambda_x)}. \tag{11}$$

Near the wall

Now that we know how to determine the spectra given a scale dependent change in convection velocity, all that remains is to determine the function $c(\lambda_x)$ (again noting that λ_x in this function is calculated using the local mean velocity). There is limited physical understanding of the mechanisms for the convection velocity change, however, it would be expected that the large-scales would move faster than the local mean at locations below the log region. That is, the large-scale features that are most energetic in the log region have a footprint near the wall which, presumably, moves with the mean velocity at the location where these structures are most energetic. It will be assumed that the smaller scales convect at the local mean velocity (DNS and experiment agree in the small scales very well). So, a function is needed that moves from the local mean velocity for the small scales to a well-defined higher velocity for the large-scales. Such a function is conceptually plotted in figure 4*b* as the dotted line. Since the pre-multiplier (equation 11) includes a derivative, a smooth function is needed, so the error function shown as the heavy, red line in figure 4*b* is used. All that remains, then, is to select a velocity for the large-scales and corner frequencies $\lambda_{xc1}, \lambda_{xc2}$ for the error function given by,

$$c(\lambda_x) = \frac{M-1}{2}\mathrm{erf}\left(\frac{1}{B}\log(\lambda_x) - D\right) + \frac{M+1}{2} = \frac{U_c}{U_l}. \quad (12)$$

Here M sets the velocity of the large-scales and B, D set the corner frequencies of the function; these constants are not functions of wall-distance in this investigation, although there is no reason they must not be. As a preliminary best fit to the data, we have chosen $M = U_{y^+=50}/U_l$, where U_l is the local mean velocity. This sets the convection velocity of the large-scales at $U_{y^+=50}$. One might argue that a velocity representative of the log region may be more appropriate, however, further work is required to establish the true speed of the large structures, and moreover, the difference in the spectra by using $M = U_{y^+=50}$ as opposed to $M = U_(y^+ = 100)$ are very small and certainly within the experimental error. Corner frequencies of $\lambda_{xc1} = 1.5h$ and $\lambda_{xc2} = 15h$ were chosen to reflect the characteristics of the large structures. Figure 4*b* illustrates the improvemed agreement in the near-wall spectra using the modified convection velocity (the dotted line is the orignal spectra, whereas the solid blue line represents the spectra with modified convection velocity). Similar improvement is noted up to $y^+ = 50$ where the convection velocity modification ceased (since this is the point where the local mean velocity is equal to the chosen convection velocity of the large structures).

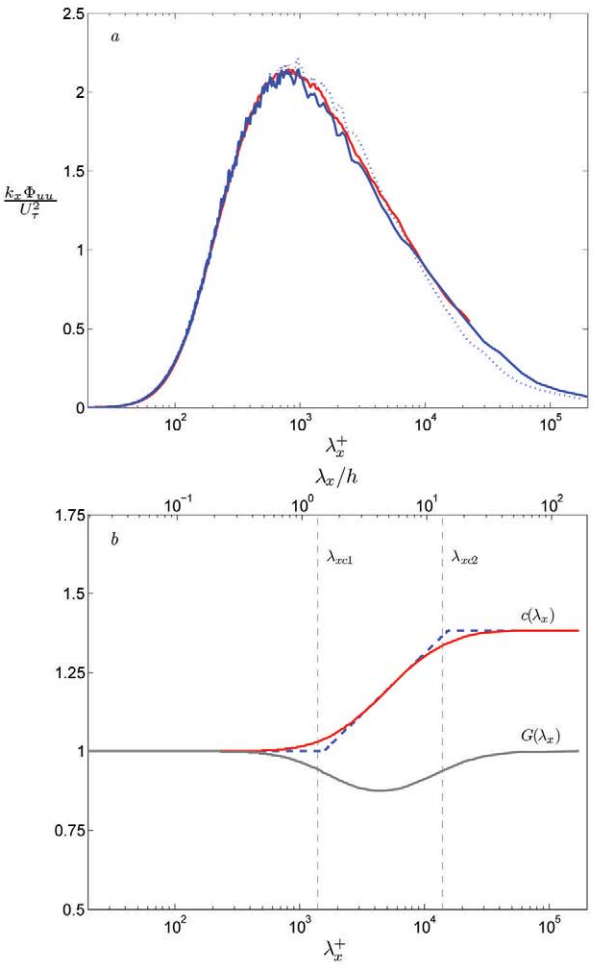

Figure 4: (*a*) Pre-multiplied spectra with modified convection velocity at $y^+ = 15$. The dotted line is the spectra calculated with local mean as the convection velocity for all scales. (*b*) Plots of the convection velocity modification, $c(\lambda_x)$ and energy redistribution function, $G(\lambda_x)$ for $y^+ = 15$.

Log region

The major discrepancy between the experimental and numerical data was found in the log region. It is possible that this is also due to convection velocity issues. Unfortunately, in this case there is no obvious physical mechanism to guide the choice of convection velocity modification. At least near the wall, one could argue that the large-scales move faster than the local mean (as above). In the log region, however, it was expected that the large structures convect at the local mean velocity. Nevertheless, a convection velocity function can be determined to collapse the experiment and the DNS. This function is identical in form to equation 12, only with quite different constants: $M = U_{y=0.25h}$, $\lambda_{xc1} = 7h$ and $\lambda_{xc2} = 25h$. The convection velocity modification (see figure 5*a*) is therefore rather sharp, but has the desired effect, as seen in figure 5*b*. Again, similar improvement is seen throughout the log and wake regions until $y = 0.25h$, at which point the local mean velocity equals the assumed convection velocity of the large-scales.

Since the physical correctness of this modified convection velocity in the log and lower-wake regions is uncertain, the conclusion from this subsection can only be: it is possible to reconcile the DNS and experimental spectra with a feasible convection velocity modification. The result that the two data sets can be made to match so well with such a simple convection velocity function is surprising and is the subject of an ongoing investigation by the authors.

The overall improvement in spectra owing to the modifications proposed here is shown more clearly in the spectra map of figure 6. Within the considerable variability of spectra calculations from wall-turbulence velocity measurements, the agreement is excellent. The only remaining discrepancy of note is in the near-wall, small scales where the DNS has more energy. This is undoubtedly due to the spatial averaging of the hot-wire, which was also responsible for the reduced peak turbulence intensity in the experimental data.

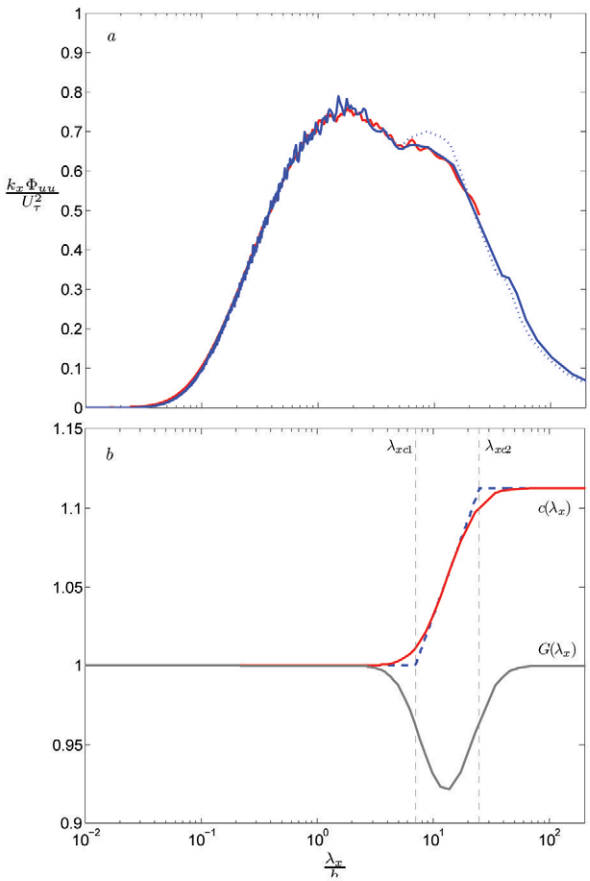

Figure 5: (a) Pre-multiplied spectra with modified convection velocity at $y^+ = 140$. The dotted line is the spectra calculated with local mean as the convection velocity for all scales. (b) Plots of the convection velocity modification, $c(\lambda_x)$ and energy redistribution function, $G(\lambda_x)$ for $y^+ = 140$.

CONCLUSION

The first known detailed comparison of streamwise velocity analysis from DNS and experimental turbulent channel flow has been conducted. The experimental data were taken by the authors and are of the highest quality. Comparisons of mean statistics show excellent agreement between the data sets, instilling confidence in both.

Comparison of the energy spectra also showed impressive overall similarity between DNS and experiment. However, it was noted that a convection velocity correction was required near the wall for the experimental data, whereby the large-scales are assumed to be moving faster than the local mean velocity up to $y^+ = 50$. A second discrepancy between the DNS and experiment was found in the log region, where the most energetic large-scales appear attenuated in the DNS compared with experiment. It was shown that it is possible to explain this behaviour through a modification to the convection velocity in the log region — very similar to that proposed near the wall. However, the physical correctness of this convection velocity distribution is uncertain and so it is also concluded that larger box sizes could be required for more accurate DNS in the future.

The authors gratefully acknowledge the financial support of the Australian Research Council (DP055277).

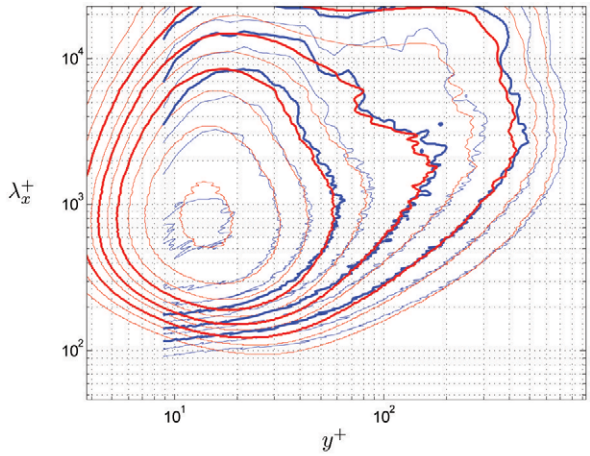

Figure 6: Spectra contour map with convection velocity modifications applied to the logarithmic and near-wall regions. Experiment in blue, DNS in red. Contour levels as in figure 3.

REFERENCES

[1] del Álamo JC and Jiménez J. "Spectra of the very large anisotropic scales in turbulent channels". *Phys. Fluids*, 2003. **15**(6), 41–44.

[2] del Álamo JC, Jiménez J, Zandonade P and Moser RD. "Scaling of the energy spectra of turbulent channels". *J. Fluid Mech.*, 2004. **500**, 135–144.

[3] Guala M, Hommema SE and Adrian RJ. "Large-scale and very-large-scale motions in turbulent pipe flow". *J. Fluid Mech.*, 2006. **554**, 521–542.

[4] Hoyas S and Jiménez J. "Scaling of the velocity fluctuations in turbulent channels up to $Re_\tau = 2003$". *Phys. Fluids*, 2006. **18**(011702).

[5] Hutchins N and Marusic I. "Evidence of very long meandering features in the logarithmic region of turbulent boundary layers". *J. Fluid Mech.*, 2007. **579**, 1–28.

[6] Hutchins N and Marusic I. "Large-scale influences in near-wall turbulence". *Phil. Trans. R. Soc. A*, 2007. **365**(1852), 647–664.

[7] Iwamoto K, Fukagata K, Kasagi N and Suzuki Y. "Dns of turbulent channel flow at $re_\tau = 1160$ and evaulation of feedback control at practical reynolds numbers". In "Proc. 5th Symp. smart Control of Turbulence, Feb 29 - Mar 2", Tokyo, 2004 .

[8] Iwamoto K, Fukagata K, Kasagi N and Suzuki Y. "Friction drag reduction achievable by near-wall turbulence manipulation at high reynolds numbers". *Phys. Fluids*, 2005. **17**(011702).

[9] Kim KC and Adrian RJ. "Very large-scale motion in the outer layer". *Phys. Fluids*, 1999. **11**(2), 417–422.

[10] Monty JP. *Developments in smooth wall turbulent duct flows*. Ph.D. thesis, University of Melbourne, 2005.